ChemComm

COMMUNICATION

View Article Online
View Journal | View Issue

Cite this: *Chem. Commun.*, 2023, 59, 13735

Received 3rd October 2023,
Accepted 24th October 2023

DOI: 10.1039/d3cc04902g

rsc.li/chemcomm

Dual emissive optically active gold nanoclusters endowed with circularly polarized phosphorescence†

Camelia Dutta, Sonia Maniappan and Jatish Kumar *

Enantiomerically pure Au nanoclusters exhibiting dual-emission corresponding to fluorescence and phosphorescence were synthesized by adopting a facile approach. Chiral luminescence was observed for the triplet emission leading to circularly polarized phosphorescence, both in solution and in solid states. The nanoclusters exhibited aggregation induced emission, and the aggregated clusters exhibited chiral phosphorescence.

Chirality is a unique geometrical property exhibited by materials on varying length scales.[1–3] Research interest towards optically active materials has seen a surge over the years due to the direct correlation between homochirality and the origin of life.[4] Emissive materials with optically active centres possess a combination of luminescence and chirality, thus exhibiting the phenomenon of circularly polarized luminescence (CPL).[5–8] Fundamental research in this field has been focused on understanding the mechanism of excited state chirality.[9,10] In this regard phosphorescent emitters with optically active centres possess an exclusive amalgamation of luminescence and chirality, thus exhibiting the phenomenon of circularly polarized phosphorescence (CPP). The systems exhibiting CPP, due to their long-lived excited states, are considered as promising for its applications in anti-glare filters and data encryption. CPP has been reported in several organic molecules and inorganic complexes, however, such an effect is rather uncommon at the nanoscale due to the difficulties in synthesizing nanomaterials that can effectively harvest longer excited state lifetimes. Atomically precise metal nanoclusters (NCs), due to their quantized energy levels and well-defined transitions, are best suited for such investigations.[13–17] The challenge is to synthesize inherently chiral clusters that exhibit intense CPL activity with prolonged excited state lifetimes. Ning Feng *et al.* probed CPP in water soluble silver NCs with a high dissymmetric factor of up to 1.05×10^{-2}.[11] Yu-Zin Kong *et al.* have set an example in this field by synthesizing bimetallic Ag–Au NCs exhibiting CPP.[12] However, comprehensive studies to unravel the mechanism of chiral luminescence in nanosystems are scarce.[18] Herein, we report CPP in a set of atomically precise gold nanoclusters (AuNCs) capped with D/L-cysteine (Fig. 1). The NCs exhibited chiral emission, both in the solution state and solid films. Moreover, the NCs showed aggregation-induced enhanced emission (AIEE), offering a unique combination of CPP and AIEE that can find excellent potential for the material to be used in display devices and bioimaging applications.

AuNCs were synthesized by mixing an aqueous solution of the Au salt with cysteine under stirring (details in ESI†).[19] The reducing ability of cysteine and strong Au–thiol binding facilitate the formation of stable NCs in solution. HRMS analysis in positive ion mode showed an intense peak at m/z = 1074.5596 a.m.u., which corresponds to a reported cluster composition of $[Au_6(C_3H_6NO_2S)_8]^{+2}$ (Fig. S1a, ESI†).[20] The residual peaks at m/z values of 975.5221 a.m.u. and 953.5448 a.m.u. match well with $[Au_6(C_3H_6NO_2S)_6]^{+2}Na$ and $[Au_6(C_3H_6NO_2S)_6]^{+2}$, respectively. Similar m/z patterns observed for the L- and D-AuNCs confirmed a similar structural composition for the NCs (Fig. S1b, ESI†). FT-IR measurements showed strong peaks confirming the presence of a chiral ligand on the NC surface (Fig. S2, ESI†). The absence of thiol

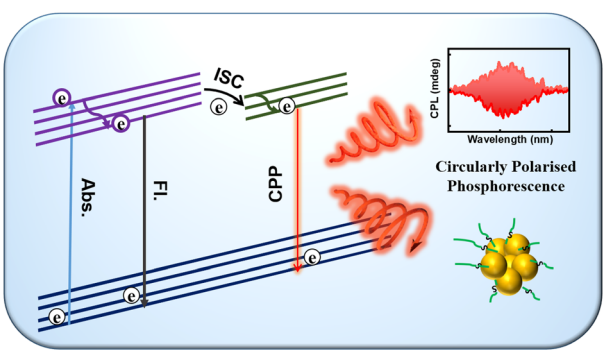

Fig. 1 Schematic representation of the CPP effect in metal NCs.

Department of Chemistry, Indian Institute of Science Education and Research (IISER) Tirupati, Tirupati–517507, India. E-mail: jatish@iisertirupati.ac.in

† Electronic supplementary information (ESI) available. See DOI: https://doi.org/10.1039/d3cc04902g

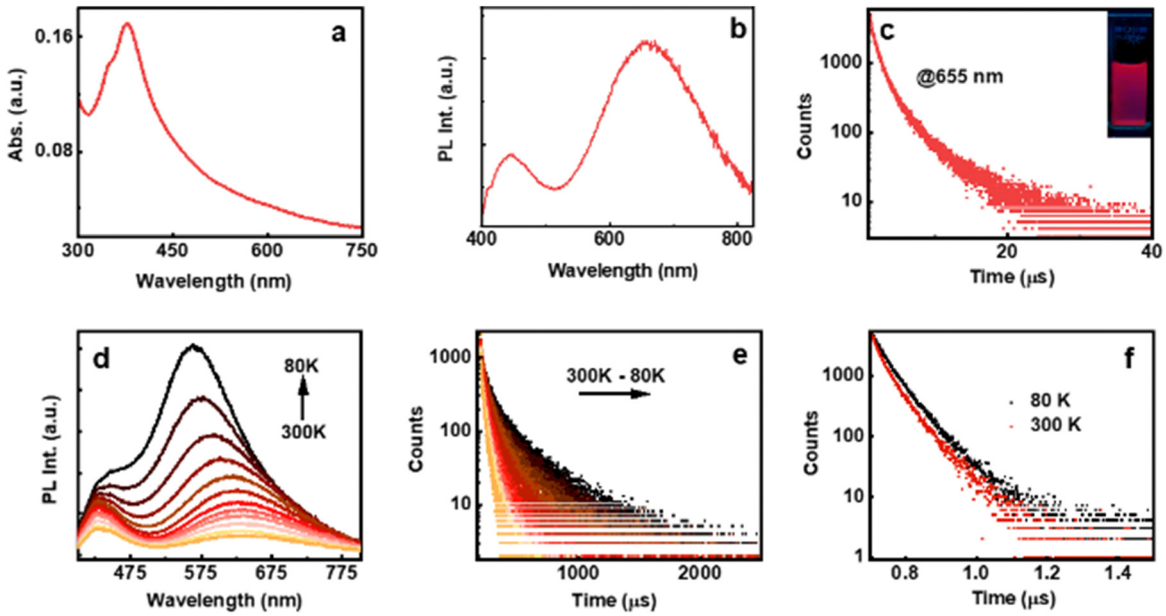

Fig. 2 (a) UV-vis and (b) emission spectra of the AuNCs dispersed in water. (c) The PL lifetime decay plot of L-AuNC solution corresponding to the red emission. The inset shows the photograph of the AuNC solution under 365 nm UV illumination. (d) Temperature dependent PL spectra of the clusters incorporated in PVA film. (e) and (f) Temperature dependent lifetime mapping corresponding to (e) 625 and (f) 430 nm photoemission.

stretching (–SH) at around 2584–2598 cm^{-1} suggested a strong Au-thiol interaction in the clusters. The stability of the AuNCs investigated at various temperatures revealed that the clusters decompose at elevated temperatures (Fig. S3 and S4, ESI†). The pH dependent investigations showed cluster stability at a highly acidic pH of 1.5 (Fig. S5, ESI†).

The optical properties of the AuNCs were investigated using UV-visible spectroscopy, which showed a characteristic peak at 377 nm with a shoulder at around 350 nm attributed to the Au $5d^{10}$-6sp inter-band transition due to the presence of ligands on the metal surface (Fig. 2a).[21] The absence of plasmonic bands in the absorption spectra or large particles in the TEM image rules out the formation of plasmonic nanoparticles (Fig. S6, ESI†). The NC formation was further established by the intense emission peaks centred at around 655 and 442 nm under 375 nm excitation (Fig. 2b). The excitation plot corresponding to both blue and red emissions matches the absorption plot pointing to the same HOMO–LUMO excitation leading to dual emission (Fig. S7, ESI†). The absolute photoluminescence quantum yields (PLQYs) of L- and D-AuNCs were estimated to be 1.27% and 1.43%, respectively. The luminescence lifetime of the L-AuNCs under ambient conditions displayed a biexponential decay with an average lifetime of 2.68 μs and 3.24 ns for the emission monitored at 655 nm and 442 nm, respectively (Fig. 2c and Fig. S8a, ESI†). A similar trend was also observed for the D-AuNCs (Fig. S8b and c, ESI†). The lifetime in microseconds is indicative of spin-forbidden transitions and demands further investigation.

To explore the origin of photoemission in the AuNCs, temperature dependent studies were carried out. Low temperature investigations on transparent self-standing composite films showed features similar to those observed in solution with an absolute PLQY of 2.2%. The NCs in polymeric films exhibited a slightly blue shifted emission relative to that in solution. For emission centred at around 625 nm, the luminescence profile in an inert environment showed a gradual increase in the intensity accompanied by a hypsochromic shift of 70 nm upon decreasing the temperature from 300 to 80 K (Fig. 2d). In contrast, no such shift was observed for the photoemission centred at 430 nm. The hypsochromic shift upon decreasing the temperature can be ascribed to the diminishing electron–phonon coupling that was dominant at higher temperature.[22,23] At room temperature, the average PL lifetime decay of the film was calculated to be 3.1 μs for emission monitored at 625 nm and 4.64 ns for emission at 430 nm (Fig. 2e and f). Interesting results were obtained for the temperature dependent lifetime measurements. The decay profiles corresponding to the 625 nm emission band exhibited a gradual increase in the lifetime with decreasing temperature reaching a value of 18.71 μs at 80 K, around 6 times enhancement compared to the value at room temperature (Fig. 2e). In contrast, negligible changes in the lifetime was observed for the decay corresponding to the 430 nm emission band (Fig. 2f).

It is evident that the lifetime in nanoseconds arises due to the spin allowed emission from the S_1 to S_0 state, hence characterized as fluorescence. In contrast, the excited state lifetime in microseconds point towards the spin forbidden transition either due to phosphorescence or due to thermally activated delayed fluorescence (TADF). To acquire a better insight into the emission mechanism, we collected the time-resolved emission spectra (TRES) of the clusters in water. The deconvoluted PL spectra with a 5 ns time interval showed a gradual descend in the blue-emitting peak after a time interval of 20 ns, whereas ascension was observed for the red-emitting peak (Fig. 3a). This is indicative of a short lived blue-emitting state and a long-lived red-emitting

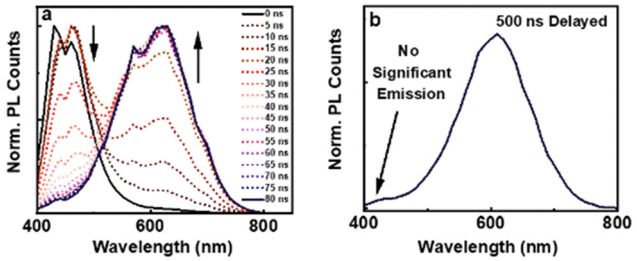

Fig. 3 (a) TRES spectra of L-AuNCs dispersed in water with a time interval of 5 ns. (b) Emission spectra with a delay time of 500 ns.

state. Similarly, the deconvoluted spectra obtained from TRES with a delay time of 500 ns showed the absence of blue-emitting peaks, validating the occurrence of room temperature red-emitting phosphorescence and blue-emitting fluorescence (Fig. 3b).[24] The deconvoluted PL spectra along with the blue shifted PL at lower temperature rule out the possibility of TADF; however, a minor contribution from the mixed singlet–triplet states due to spin-orbital coupling cannot be ruled out and needs further investigation. Selective quenching of the red emission peak in the presence of oxygen further confirms the involvement of the triplet state (Fig. S9, ESI†). It can be concluded that the PL at 430 nm arises due to the decay from the singlet and that at 625 nm primarily from the triplet. Hence, the former can be assigned as fluorescence and the latter phosphorescence.

The main focus of the project is to study the optical activity of the AuNCs. Ground state chiral investigations revealed mirror image CD profiles for the L- and D-AuNCs. The CD signals were consistent with the absorption peaks (Fig. 4a). The PL intensity and chiral nature of the clusters prompted us to investigate the excited state optical activity. Interestingly, the D- and L-AuNCs exhibited positive and negative CPL responses respectively corresponding to the red emission (Fig. 4b). The signs of CD and CPL signals were in agreement, indicating a similar nature for the transitions. A g_{lum} value of -8.1×10^{-3} was observed for the L-AuNCs and a g_{lum} value of $+6.2 \times 10^{-3}$ was observed for the D-AuNCs (Fig. S10a, ESI†). The chiral anisotropy is comparable with the typical values reported for organic systems and luminescent nanomaterials. The room temperature emission of the clusters is characterized as phosphorescence, and the observed chiral luminescence can be referred to as CPP.

Inspired by the attractive chiroptical properties of the AuNCs in solution, we investigated the CPL on a solid surface, which widens their scope for a plethora of applications. Interestingly, the AuNC incorporated PVA films exhibited mirror image CPP responses (Fig. 4c and d) with the g_{lum} values of -6.9×10^{-3} and $+5.1 \times 10^{-3}$ for the films prepared from the L- and D-AuNCs, respectively (Fig. S10b, ESI†). The CPP collected from different points by flipping and rotating the film showed consistent signals establishing the reproducibility and ruling out the possibility of any artefacts (Fig. S11, ESI†). Thus, the CPP effect in enantiomerically pure AuNCs could be established both in the solution state and free-standing films.

AIEE is an interesting phenomenon observed in a few metal clusters, which can enhance their luminescence, thereby

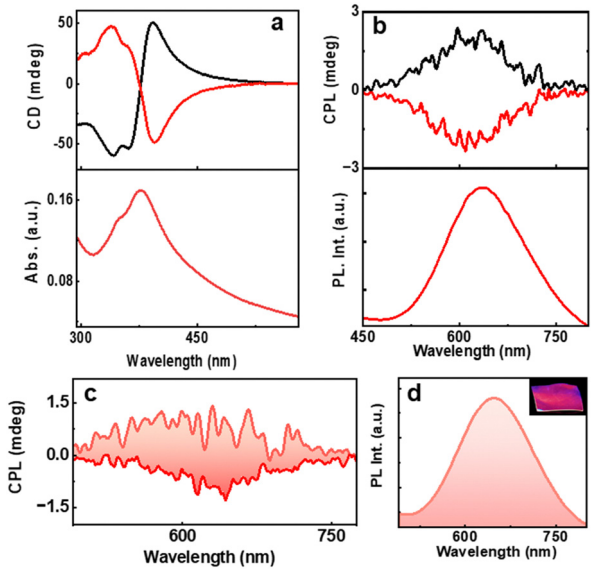

Fig. 4 (a) CD and the corresponding UV-visible spectra and (b) CPL and the corresponding PL spectra of aqueous AuNC solution. Black and red traces correspond to D- and L-AuNCs, respectively. (c) CPL and the (d) luminescence plot of the AuNC incorporated PVA film. The positive and negative CPL plot corresponds to D- and L-AuNC, respectively. The inset in 'd' shows the photograph of the film under 365 nm UV illumination.

finding a wider application in the field of light emitting materials.[25] To study the assembly of the AuNCs, the optical characteristics of the clusters were monitored in different solvents (Fig. S12, ESI†). While most solvents showed either no change or quenching, PL enhancement was observed for the NCs dispersed in acetone (Fig. 5b). The absorption spectra showed no noticeable changes in the peak position; however, broadening was observed due to aggregation and increased scattering (Fig. 5a). The aggregates exhibited a PLQY of 4.57%, a 3-fold enhancement relative to the monomeric clusters. Acetone being a weakly polar solvent compared to water disrupts the hydration shell of the monomeric AuNCs, thus inducing destabilization and charge neutralization leading to aggregation.[26] The self-assembly led to the formation of larger aggregates of irregular morphology as evident from the TEM images (inset Fig. 5a). The FT-IR spectra of the assembled structures showed a less intense N–H bending along with the enhanced amide stretches suggesting the formation of amide linkages during aggregation (Fig. S13b, ESI†). The aggregated NCs exhibited a biexponential PL decay with an average lifetime of 1.17 μs and 2.87 ns for the emission at 650 and 430 nm, respectively (Fig. 5c and Fig. S14, ESI†). While the aggregated clusters showed enhanced PL, no noticeable enhancement was observed in their chiral properties (Fig. S15, ESI†). Chirality in metal NCs arises due to the discrete arrangement of the ligands around the metal centre. Aggregation can result in an alteration of the fine structure, thereby affecting the chirality. The CPL plot for the enantiomeric NCs showed mirror image signals analogous to the monomeric clusters; however, the spectra were relatively noisy due to the settling of larger aggregates (Fig. 5d). The aggregated clusters exhibited an average g_{lum}

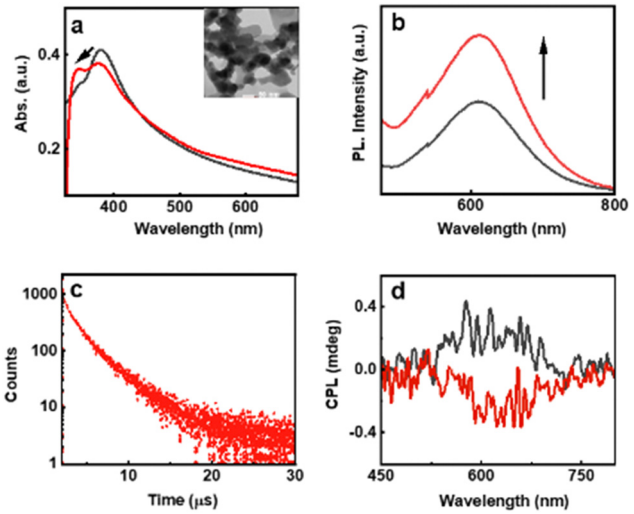

Fig. 5 (a) UV-vis and (b) PL spectra of AuNCs in water (black trace) and acetone (red trace). (c) Lifetime decay of clusters in acetone monitored at the red emitting PL maxima. (d) CPL plot of AuNC assemblies in acetone. Black and red traces correspond to D- and L-AuNCs. The inset in 'a' shows the TEM image of the aggregated NCs.

values of $+9 \times 10^{-3}$ and -7×10^{-3} for the assemblies formed from the D- and L-AuNCs, respectively (Fig. S16, ESI†).

Phosphorescence in the monomeric NCs inspired us to investigate a similar effect in the aggregated state. Temperature dependent emission of PVA film incorporated with aggregated NCs showed an effect analogous to the monomeric NCs (Fig. S17a, ESI†). The excited state lifetime showed an enhancement from 2.33 to 9.67 μs upon lowering the temperature (Fig. S17b, ESI†). Likewise, emission at 430 nm exhibited no noticeable change in the lifetime with temperature (Fig. S17c, ESI†). Hence, the observed chiral emission of the red peak could be assigned primarily to the CPP effect, both in the monomeric and aggregated AuNCs.

In summary, we have successfully synthesized a pair of enantiomeric AuNCs using cysteine ligands. The long PL lifetime in conjunction with the chirality of the clusters led to CPP, a rather unusual observation in metal NCs. Chiral emission could be demonstrated in the free-standing polymeric films of the NCs. The solvent induced assembly of the AuNCs assisted in modulating their optical properties through AIE. The basic understanding of the mechanism of chiral luminescence in the NCs can open newer avenues for fundamental research on a similar class of nanomaterials. The observation of CPP and AIE in the AuNCs has led to exciting properties opening wider possibilities for their application in security tags, data encryption and light emitting devices.

J. K. acknowledges financial support from CSIR India (Grant No. 01(3029)/21/EMR-II) and STARS, MoE, Govt. of India (Project ID: 2023-0490). C. D. acknowledges Prime Minister's Research Fellowship, Govt. of India for the fellowship and funding. S. M. acknowledges DST INSPIRE for the fellowship. The authors acknowledge IISER Tirupati for providing research facilities.

Conflicts of interest

There is no conflict of interest to declare.

Notes and references

1 Y. Wang, J. Xu, Y. Wang and H. Chen, *Chem. Soc. Rev.*, 2013, **42**, 2930–2962.
2 J. B. Youatt and R. D. Brown, *Science*, 1981, **212**, 1145–1146.
3 S. Maniappan, C. Dutta, D. M. Solís, J. M. Taboada and J. Kumar, *Angew. Chem., Int. Ed.*, 2023, e202300461.
4 W. Ma, L. Xu, A. F. de Moura, X. Wu, H. Kuang, C. Xu and N. A. Kotov, *Chem. Rev.*, 2017, **117**, 8041–8093.
5 A. Warshel Schlessinger, *Chem. Phys. Lett.*, 1974, **28**, 380–383.
6 S. Maniappan, K. L. Reddy and J. Kumar, *Chem. Sci.*, 2023, **14**, 491–498.
7 A. Das, S. Ghosh and S. J. George, *Angew. Chem., Int. Ed.*, 2023, e202308281.
8 K. L. Reddy, J. P. Mathew, S. Maniappan, C. Tom, E. Shiby, R. K. Pujala and J. Kumar, *Nanoscale*, 2022, **14**, 4946–4956.
9 F. S. Richardson and J. P. Rlehl, *Chem. Rev.*, 1986, **86**, 1–16.
10 J. Kumar, T. Kawai and T. Nakashima, *Chem. Commun.*, 2017, **53**, 1269–1272.
11 N. Feng, Z. Wang, D. Sun, P. Sun, X. Xin, X. Cheng and H. Li, *Adv. Opt. Mater.*, 2022, **10**, 2102319.
12 Y. J. Kong, J. H. Hu, X. Y. Dong, Y. Si, Z. Y. Wang, X. M. Luo, H. R. Li, Z. Chen, S. Q. Zang and T. C. Mak, *J. Am. Chem. Soc.*, 2022, **144**, 19739–19747.
13 R. Jin, *Nanoscale*, 2010, **2**, 343–362.
14 Y. Tao, M. Li, J. Ren and X. Qu, *Chem. Soc. Rev.*, 2015, **44**, 8636–8663.
15 S. Knoppe and T. Burgi, *Acc. Chem. Res.*, 2014, **47**, 1318–1326.
16 W. Ishii, Y. Okayasu, Y. Kobayashi, R. Tanaka, S. Katao, Y. Nishikawa, T. Kawai and T. Nakashima, *J. Am. Chem. Soc.*, 2023, **145**, 11236–11244.
17 S. R. Biltek, S. Mandal, A. Sen, A. C. Reber, A. F. Pedicini and S. N. Khanna, *J. Am. Chem. Soc.*, 2013, **135**, 26–29.
18 C. Dutta, S. Maniappan and J. Kumar, *Chem. Sci.*, 2023, **14**, 5593–5601.
19 Y. S. Borghei, M. Hosseini and M. R. Ganjali, *Curr. Nanosci.*, 2017, **13**, 610–615.
20 K. Salorinne, R. W. Man, P. A. Lummis, M. S. A. Hazer, S. Malola, J. C. H. Yim, A. J. Veinot, W. Zhou, H. Häkkinen, M. Nambo and C. M. Crudden, *Chem. Commun.*, 2020, **56**, 6102–6105.
21 P. Rodriguez-Zamora, C. A. Cordero-Silis, G. R. Garza-Ramos, B. Salazar-Angeles, J. C. Fabila, F. Buendia, L. O. Paz-Borbon, G. Diaz and I. L. Garzon, *Small*, 2021, **17**, 2004288.
22 Y. P. Varshni, *Physica*, 1967, **34**, 149–154.
23 N. M. Ravindra and V. K. Srivastava, *J. Phys. Chem. Solids*, 1979, **40**, 791–793.
24 S. Sharma, S. Das, K. Kaushik, A. Yadav, A. Patra and C. K. Nandi, *J. Phys. Chem. Lett.*, 2023, **14**, 8979–8987.
25 Z. Luo, X. Yuan, Y. Yu, Q. Zhang, D. T. Leong, J. Y. Lee and J. Xie, *J. Am. Chem. Soc.*, 2012, **134**, 16662–16670.
26 Z. Ma, G. Gao, Z. Luo, X. Tang and T. Sun, *J. Phys. Chem. C*, 2019, **123**, 24973–24978.

